Materials Science Communication

Analysis of valence electron structures (VES) of intermetallic Fe₃Al compounds

Yin Yansheng [a], Wang Wen Xiang [b], Shi Zhongliang [c]

[a] *Department of Materials Science Engineering, Dalian University of Technology, Dalian 116023, China*
[b] *Daqing Petrochemical Design Institute, Daqing 163714, China*
[c] *Shanghai Jiaotong University, Shanghai 200030, China*

Abstract

Based on the empirical electron theory of solids and molecules, analysis of valence electron structures is made on Fe₃Al intermetallic compounds. The bonding complex model of the DO₃ cell is set up. Some preliminary attempts to discover the relationship between alloy composition, structure and properties and the Fe₃Al alloy phase valence electron structure are presented.

Keywords: Valence electrons; Intermetallic compounds; Bonding complexes

1. Introduction

When electrons are fully arranged in the atomic internal crust, the properties of the atoms mainly depend upon the outer valence electron structure (VES). When a quantity of atoms gather together, changes in the VES of the atom in a polymerized state will occur. The properties of a material are closely related to the VES of the atoms in the polymerized state, which is a reflection of the relationship between the material's composition, structure and properties. However, calculation of the VES of an atom in a condensed state is not well solved by the quantum mechanics theory of solids over a long period of time; therefore the essential relationship between a material's composition, structure and properties and the VES is not yet known. The empirical electron theory of solids and molecules formulated by Yu includes a method for calculating the populations of atomic VES, which makes it possible to calculate the alloy phase VES [1].

According to the performance criteria required by a material, the defined composition and alloying technology are given by theory, which is being developed in materials science. Past research efforts mostly placed emphasis on the effect of the atomic structural changes of a material and alloy on their composition and prop-

erties. Presently, more and more researchers are paying attention to the electron theory in material composition design.

It should be said that the electron theory is established first on the research and study of metallic materials, and is widely used in materials science and other fields, particularly semiconductor materials, which has effectively improved the development of many new materials and fresh technologies. However, the electron theory has made relatively slow progress in the study of metallic materials. The study of metals and alloys is not beyond the scope of atom arrangement and its change rule; the effect and behaviour of alloy elements in alloy materials has not yet eliminated the empirical range of test measurements and summing up the regularity. The costly fried-dish-type method is still a major method in alloy composition design. One main reason for this situation is that materials science has not yet gone into the field of electron structures, and the essential relationship between the VES of atoms in a condensed state and alloy composition, structure and properties has not yet been discovered. The relative sluggish progress of electron theory in the study of metallic materials has complex causes. Because metal alloys are complex systems, they are more difficult to deal with strictly in theory. A simple and effective way to probe

the electron theory of materials science is from the viewpoint of experimental fact, using the method of combining theory with practice.

Alloy theoretical composition design according to valence electron theory is carried out mainly based on the analysis of the atomic state hybridization and bond distance difference. In light of the energy band theory of quantum mechanics, atomic energy levels gradually widen and become energy bands when atoms are in contact with each other in solids. While the increasing height of the atomic energy band largely exceeds the energy level of some excited state, the overlap of atomic states which is called an atomic hybridized state, is built up [2]. The atomic hybridized state defines the atomic covalent electron number, the lattice electron number, the magnetic electron number and the dummy paired electron number. It may be determined from this that the bonding complex in a crystal is known. These pieces of information on VES provide a quantitative basis for the study of many important subjects, such as the properties of metallic materials, and phase changes of the solid state.

Fe$_3$Al intermetallic compounds are one of the main materials being actively studied presently in the international materials field, but so far no theoretical reports on alloy composition design have been presented concerning the alloying effect on Fe$_3$Al. This paper is intended to set up the VES of binary Fe$_3$Al alloy phase and to report a preliminary study of the Fe$_3$Al strong toughening mechanism.

2. Fe$_3$Al cell structures

The DO$_3$ cell structure of Fe$_3$Al is shown in Fig. 1. One DO$_3$ cell consists of four A2 (b.c.c.) and four B2 cells, and belongs to the f.c.c. lattice. Its lattice constant a is twice a_0 (a_0 is the B2 lattice constant, equal to 2.90 Å). In a DO$_3$ cell, the Fe atoms located at the centers of the six surfaces, the Fe atoms located in
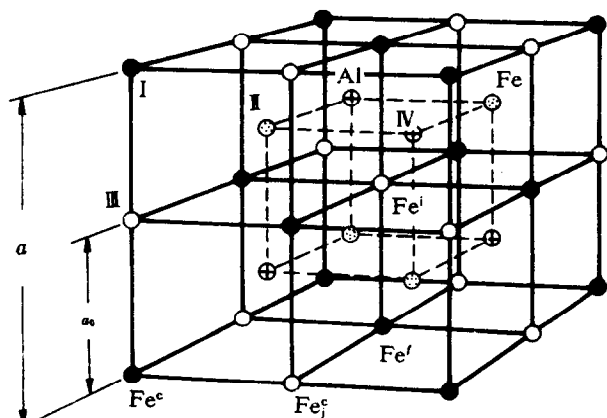
the center of cell interior, the Al and Fe atoms at the diagonal 1/4 and 3/4 of the cell interior, the Fe atoms in the center of the cell edge and the Fe atoms at the top of the cell are expressed separately as Fe^f, Fe^i, Al, Fe, Fe^c_j and Fe^c. The bonding complex, the experimental covalent bond distance D_{na} and the identity bond number I_a in the Fe$_3$Al unit cell are shown in Table 1. When the bond distance is set, the bond complex formula, where the bond distance exceeds $\sqrt{3}a_0$, is ignored in the text. Because the bond distance is too long, its bonding effect is rather weak. In the text, Fe atoms with various symbols are regarded as similar atoms. D_{na} is the covalent bond distance for an individual atom, which can be determined by solid geometry. The identity bond number I_a can be calculated using the formula in Ref. [3].

2.1. Calculation of theoretical covalent bond distance $\tilde{D}_{na}$

2.1.1. Establishment of log r_a equation

In general, the calculation formula of D_{na} is [3,4]

$$D_{na} = R_u(I) + R_v(I) - \beta \log n_a$$

where u and v can be either like or unlike atoms; n_a is expressed as covalent electron pairs and a as different bonds (a = A, B, C, ...). For a metal, β is a constant, taken to be 0.6 [3]. $R(I)$ is the single-bond semi-distance of an atom. If this formula is used for the Fe$_3$Al cell, the expressions of each bond distance in Table 1 are as follows:

Table 1
The experimental covalent bond distances and the identity bond numbers of the binary Fe$_3$Al unit cell

Bond	D_{na} (Å)	I_a
Fe^i–Fe^f = A	$D_{nA} = a_0$	$I_A = 12$
Fe^i–Fe^c = B	$D_{nB} = \sqrt{3}a_0$	$I_B = 16$
Fe^i–Fe^c_j = C	$D_{nC} = \sqrt{2}a_0$	$I_C = 24$
Fe^i–Fe = D	$D_{nD} = (\sqrt{3}/2)a_0$	$I_D = 8$
Fe^i–Al = E	$D_{nE} = (\sqrt{3}/2)a_0$	$I_E = 8$
Fe^c–Fe^f = F	$D_{nF} = \sqrt{2}a_0$	$I_F = 24$
Fe^c–Fe^c_j = G	$D_{nG} = a_0$	$I_G = 12$
Fe^c_j–Fe^c_j = J	$D_{nJ} = \sqrt{2}a_0$	$I_J = 24$
Fe^c_j–Fe^f = K	$D_{nK} = a_0$	$I_K = 24$
Fe^c_j–Fe = L	$D_{nL} = (\sqrt{3}/2)a_0$	$I_L = 24$
Fe^c_j–Al = M	$D_{nM} = (\sqrt{3}/2)a_0$	$I_M = 24$
Fe^f–Fe^f = N	$D_{nN} = \sqrt{2}a_0$	$I_N = 24$
Fe^f–Fe = P	$D_{nP} = (\sqrt{3}/2)a_0$	$I_P = 24$
Fe^f–Al = Q	$D_{nO} = (\sqrt{3}/2)a_0$	$I_O = 24$
Fe–Fe = S	$D_{nS} = (\sqrt{3}/2)a_0$	$I_S = 12$
Fe^c–Fe = X	$D_{nX} = (\sqrt{3}/2)a_0$	$I_X = 8$
Fe^c–Al = Y	$D_{nY} = (\sqrt{3}/2)a_0$	$I_Y = 8$
Fe–Al = T	$D_{nT} = a_0$	$I_T = 24$
Al–Al = U	$D_{nU} = \sqrt{2}a_0$	$I_U = 12$

Fig. 1. DO$_3$ cell of Fe$_3$Al.

$$\bar{D}_{nA} = R_{Fe^i}(I) + R_{Fe^f}(I) - \beta \log n_A$$

$$\bar{D}_{nB} = R_{Fe^i}(I) + R_{Fe^c}(I) - \beta \log n_B$$

$$\cdots \quad \cdots$$

$$\bar{D}_{nU} = 2R_{A1}(I) - \beta \log n_U \tag{1}$$

Subtracting both sides of the first formula from both sides of the other formulas in turn, the following can be obtained:

$$\log \gamma_B = [\bar{D}_{nA} - D_{nB}]/\beta + [R_{Fe^c}(I) - R_{Fe^f}(I)]/\beta$$

$$\log \gamma_C = [\bar{D}_{nA} - \bar{D}_{nC}]/\beta + [R_{Fe^j}(I) - R_{Fe^f}(I)]/\beta$$

$$\cdots \quad \cdots$$

$$\log \gamma_U = [\bar{D}_{nA} - \bar{D}_{nU}]/\beta$$
$$+ [2R_{A1}(I) - R_{Fe^i}(I) - R_{Fe^f}(I)]/\beta \tag{2}$$

In this way, 18 equations are set up for the 19 covalent bonds. The value of γ_a reflects the relative values $n_B \ldots n_U$ with respect to n_a on each bond of $D_{nB} \ldots D_{nU}$.

2.1.2. The equation for n_a

One Fe^c atom, one Fe^i atom, three Fe^f atoms, three Fe^c_j atoms, four Fe atoms and four Al atoms are contained in one DO_3 cell of Fe_3Al. The number of covalent electrons of atoms contained in the unit cell is as follows:

$$\Sigma n_c = n_c^{Fe^c} + 3n_c^{Fe^f} + 3n_c^{Fe^cj} + n_c^{Fe^i} + 4n_c^{Fe} + 4n_c^{A1} \tag{3}$$

From the distribution of these covalent electrons building covalent electron pairs on each covalent bond, the total number of covalent electrons in the cell can also be expressed as

$$\Sigma n_c = \Sigma I_a n_a = n_A\{I_A + I_B\gamma_B + \ldots + I_U \gamma_U\} = n_A\Sigma I\gamma \tag{4}$$

Then

$$n_A = \Sigma n_c/\Sigma I\gamma \tag{5}$$

Using the relation $n_a = n_A\gamma_a$, the common electron pairs n_a on U covalent bonds can be obtained.

2.1.3. Calculation of the theoretical bond distance $\bar{D}_{na}$

From the above expression $\bar{D}_{na}$ of each bond distance, the individual theoretical bond distance equations were obtained and are listed below:

$$\bar{D}_{nA} = R_{Fe^i}(I) + R_{Fe^f}(I) - \beta \log n_A$$

$$\bar{D}_{nB} = R_{Fe^i}(I) + R_{Fe^c}(I) - \beta \log n_B$$

$$\cdots \quad \cdots$$

$$\bar{D}_{nU} = 2R_{A1}(I) - \beta \log n_U$$

when

$$|\Delta D_{na}| \leqslant \begin{vmatrix} D_{nA} - \bar{D}_{nA} \\ D_{nB} - \bar{D}_{nB} \\ \cdots \quad \cdots \\ D_{nU} - \bar{D}_{nU} \end{vmatrix}$$

where ΔD_{na} is the bond distance difference.

This can be considered as the actual state of selected hybrid step coincidence atoms in the DO_3 cell. In the $\log \gamma_a$ equation set, experimental covalent bond distances are given in Table 1.

The single bond semi-distance $R(I)$ and each atomic valence electron number n_a can be found from the binary hybridization list of Fe [3] and the binary hybridization list of Al [5], so that the conditions for using a computer to calculate the VES of Fe and Al are derived. While performing calculations, the data in the binary hybridization list of Fe [3] and the binary hybridization list of Al can be scanned using a computer so as to find all resolutions that satisfy the above requirements of accuracy. A block diagram of the calculation program is not shown. After analysis and comparison with the calculated results, it can be determined that Fe^c, Fe^i, Fe^f, Fe^c_j, Fe and Al occur separately in 8, 16, 5, 16, 9 and 6 steps; therefore the VES of Fe and Al can be established. The value of n_a for each bond in the VES is listed in Table 2. It can be rearranged in the order of the n_a values.

3. Results and discussion

The analysis of the calculated results (Table 2) of the VES of the Fe_3Al cell unit can be summarized as follows:

Table 2
The valence electronic structure of the binary Fe_3Al unit cell [a]

Bond	I_a	D_{na}	$\bar{D}_{nA}$	n_a	ΔD_{na}
Fe^c_j–Al = a	24	$(\sqrt{3}/2)a_0$	2.473	0.6250	0.0478
Fe^c_j–Fe = b	24	$(\sqrt{3}/2)a_0$	2.473	0.5381	0.0478
Fe^c–Al = c	8	$(\sqrt{3}/2)a_0$	2.473	0.4580	0.0478
Fe^i–Al = d	8	$(\sqrt{3}/2)a_0$	2.473	0.4705	0.0478
Fe^f–Al = e	24	$(\sqrt{3}/2)a_0$	2.473	0.4705	0.0478
Fe^i–Fe = f	8	$(\sqrt{3}/2)a_0$	2.473	0.4015	0.0478
Fe^f–Fe = g	24	$(\sqrt{3}/2)a_0$	2.473	0.4015	0.0478
Fe^c–Al = j	8	$(\sqrt{3}/2)a_0$	2.473	0.3944	0.0478
Fe–Al = k	24	a_0	2.863	0.1358	0.0478
Fe^c–Fe^c_j = l	12	a_0	2.863	0.1211	0.0478
Fe^c_j–Fe^f = m	24	a_0	2.863	0.9361×10^{-1}	0.0478
Fe^i–Fe^f = n	12	a_0	2.863	$0.7.47 \times 10^{-1}$	0.0478
Al–Al = p	12	$\sqrt{2}a_0$	4.0676	0.1548×10^{-2}	0.0478
Fe^c_j–Fe^c_j = q	24	$\sqrt{2}a_0$	4.0676	0.1220×10^{-2}	0.0478
Fe–Fe = s	12	$\sqrt{2}a_0$	4.0676	0.1148×10^{-2}	0.0478
Fe^i–Fe^c_j = x	24	$\sqrt{2}a_0$	2.473	0.9185×10^{-3}	0.0478
Fe^c–Fe^f = y	24	$\sqrt{2}a_0$	2.473	0.8942×10^{-3}	0.0478
Fe^f–Fe^f = t	24	$\sqrt{2}a_0$	2.473	0.6914×10^{-3}	0.0478
Fe^i–Fe^c = u	16	$\sqrt{3}a_0$	4.9922	0.2573×10^{-4}	0.0478

[a] For Fe^c, Fe^i, Fe^f, Fe^c_j, Fe and Al, the hybridized state numbers are 8, 16, 5, 16, 9 and 6, respectively.

Table 3
The valence electronic structure of the FeAl unit cell

a_0	Fe:	$n_{\tau18}$	n_{L18}	n_{c18}	$R_{18}(I)$	Al:	$n_{\tau3}$	n_{13}	n_{c3}	$R_3(I)$
2.909 Å		6	0	6	1.081 Å		3	1.828	1.172	1.90 Å
	I_a	D_{na}	$\bar{D}_{na}$	ΔD	na		I_a	D_{na}	$\bar{D}_{na}$	ΔD
$D_{uv}(n_A)$	16	$(\sqrt{3}/2)a_0$	2.5239	0.0064	0.3789	$D_{VV}(n_c)$	6		2.9090	2.9136	0.0046
$D_{uu}(n_B)$	6	a_0	2.9136	0.0046	0.0559		$n_a=0.1290$				

(1) In the DO_3 cell, the Al atom is in the 6-step hybridized state, and the individual Fe atoms (Fe^c, Fe^f, Fe^c_j, Fe^i and Fe) are in the binary hybridized 8-, 16-, 5-, 16- and 9-step states, respectively.

(2) There are six kinds of stronger bonds, i.e., Fe^c_j–Al, Fe^i–Al, Fe^f–Al, Fe^c_j–Fe, Fe^i–Fe and Fe^c–Fe. There are 24 strongest bonds of Fe^c_j–Al on which the covalent electron pairs are as high as 0.625.

(3) In the DO_3 cell interior, the bonding complex Fe–Fe, Al–Al is very weak, and the n_a value is negligible.

(4) In the case of identical bond distances, the Fe–Al bond of covalent electron pairs is stronger than the Fe–Fe bond, i.e., unlike-atom combined bonds are stronger than like-atom combined bonds.

According to the Fe–Al system phase diagram, Fe_3Al, whose composition is Fe–25at.%Al, is twice subject to an ordering balance transition after condensation during balance and cooling. At a temperature of 850 °C, Fe_3Al is in the disordered b.c.c. structure. As the temperature is decreased below 850 °C, the disordered b.c.c. structure is converted into the ordered B2 structure (the B2 structure was originally completely ordered, but it is in a semiordered state because of the deviation of the Fe_3Al composition from the FeAl standard composition of the B2 structure), which is the first ordering transition. When the temperature is lowered to about 540 °C, the semidisordered B2 structure is converted into a completely ordered DO_3 structure. The analyses on the VES of α-Fe with b.c.c. structure and FeAl with B2 structure were made by Yu and Liu. The results of the latter are listed in Table 3 [6].

It is not difficult to see, after analyzing the data shown in Table 3 that in both α-Fe [3] with b.c.c. structure or FeAl with B2 structure, the strong bonds are Fe–Al in the crystalline $\langle 111 \rangle$ direction, whereas the weak bonds are Fe–Fe and Al–Al in the crystalline $\langle 100 \rangle$ direction. Therefore the body-centered-cubic metal $\langle 100 \rangle$ crystalline direction is called the soft direction [7]. The general body-centered-cubic cleavage plane is the {100} surface. The analysis of the VES of Fe_3Al, which is twice subject to the b.c.c.–B2–DO_3 transition, in this paper shows that in the binary Fe_3Al cell the strongest six kinds of bonds (Table 2) are also

in the $\langle 111 \rangle$ direction, whereas the bonds in the $\langle 100 \rangle$ crystalline direction are obviously much weaker than those in the $\langle 111 \rangle$ direction. It can be seen from this that although the Fe_3Al ordering transition makes the crystalline structure change twice, the basic characteristics of anisotropy still remain unchanged. Various reports have shown that the fracture topography of binary Fe_3Al is a complete cleavage fracture. Sun et al. [6], using X-rays and the Laue method, showed that the crystallographic direction of the cleavage plane on a fracture is $\langle 100 \rangle$; these results agree with those for the VES in this paper.

McKamey et al. [8] first found that upon adding Cr to Fe_3Al, the room-temperature plasticity and tensile strength of Fe_3Al can be significantly improved, and its fracture topography is changed from 100% cleavage fracture to mixed-type fracture, approximately half cleavage and half intergranular. Their corollary is that addition of Cr improves the cleavage fracture strength of Fe_3Al so as to reach about the same level as the intergranular fracture strength and raise the plasticity, while building the above mixed-type fracture. If this corollary is right, the addition of Cr will inevitably act in the cell to strengthen covalent electron pairs in the $\langle 100 \rangle$ direction. Work on this aspect is now under way.

4. Brief summary

The analysis and calculation made on the VES of binary Fe_3Al in intermetallic compounds with the empirical electron theory show that in the Fe_3Al unit cell with DO_3 structure, Fe atoms are in hybridized states of 8, 16, 5, 16 and 9 steps, whereas the Al atoms are in a 6-step hybridized state. Covalent bonds of the unlike-atom pair (Fe–Al) are stronger than those of same-atom pairs (Fe–Fe, Al–Al), and strong bonds are mainly distributed in the crystalline $\langle 111 \rangle$ direction. The $\langle 100 \rangle$ crystalline direction is a soft direction. For polycrystalline Fe_3Al material, the alloying direction should be the covalent bonds in the $\langle 100 \rangle$ direction, which will strengthen the crystal structure.

References

[1] R.H. Yu, Empirical electron theory of solids and molecules, *Sci. Bull.*, *23* (1978) 217–224.

[2] R.H. Yu, The analysis of valence electron and magnetic distance structures of α-Fe, γ-Fe and Fe$_4$N, *Acta Metall. Sin.*, *3* (1982) 336.

[3] Z.L. Liu, *Alloy VES and Composition Design*, Jilin Science and Technology Publishing House, Changchun, China, 1990, pp. 6–13.

[4] L. Pauling, *Phys. Rev.*, *54* (1938) 899.

[5] R.H. Yu, The analysis on VES of aluminum–magnesium binary metallograph α-, δ- and γ-Al$_{12}$Mg$_{17}$ phases, *Nat. Sci. J. Jilin Univ.*, *4* (1979) 55–57.

[6] Y.S. Sun, J. Guo, L. Zhang and J. Zhang, The effect of Ce and Cr on Fe$_3$Al mechanics property at room temperature, *Acta Metall. Sin.*, *4* (27) (1991) A257–262.

[7] D.A. Porter and K.E. Easterling, *Phase Transformation in Metals and Alloys*, Alden, Oxford, 1981.

[8] C.G. McKamey, J.A. Horton and C.T. Liu, *J. Mater. Res.*, *4* (1989) 1156.